Performance of Multi-Antenna Signaling Strategies Using Dual-Polarized Antennas: Measurement Results and Analysis

Rohit U. Nabar[1)], *Vinko Erceg*[2)], *Helmut Bölcskei*[3)] *and Arogyaswami J. Paulraj*[1)]

[1)] Information Systems Laboratory, Stanford University
Packard 228, 350 Serra Mall, Stanford, CA 94305
Phone: (650)-497-9065, Fax: (650)-723-8473, email: {nabar, apaulraj}@stanford.edu
[2)] Iospan Wireless Inc., 3099 N. First Street, San Jose, CA 95134.
email: verceg@iospanwireless.com
[3)]Department of Electrical Engineering, University of Illinois at Urbana-Champaign
126 Computing Systems Research Lab, 1308 W. Main, Urbana, IL 61801
email: bolcskei@comm.csl.uiuc.edu

Abstract

Multiple-input multiple-output (MIMO) wireless systems employ spatial multiplexing to increase spectral efficiency or transmit diversity techniques to improve link reliability. The performance of these techniques is highly dependent on channel statistics which in turn depend on antenna spacing and richness of scattering. The use of dual-polarized antennas is a cost and space effective alternative where two spatially separated antennas can be replaced by orthogonally polarized antenna elements. In this paper, we use fixed-wireless experimental data collected in a typical suburban environment at 2.5 GHz to investigate the performance of spatial multiplexing and transmit diversity (Alamouti scheme) for a dual-polarized antenna setup. Channel measurements were conducted over a cell of radius 7 km and channel statistics such as K-factor, cross-polarization discrimination (XPD) and fading signal correlation were extracted from the gathered data. At each location, different combinations of these parameters yield different performance of spatial multiplexing and the Alamouti scheme. We evaluate the performance of the two transmission techniques in terms of average bit error rate for a fixed data rate and signal to noise ratio as a function of distance from the base-station using previously developed performance analysis techniques for narrowband polarization diversity based MIMO links. The results indicate that proper selection of the transmission mode through feedback, if possible, can lead to improvements in the bit error rate by several orders of magnitude. Furthermore, the results hint to the existence of a preferred-mode switching distance within a cell – above/below which one mode of transmission is generally preferred.

Keywords

MIMO, measurements, polarization diversity, spatial multiplexing, Alamouti scheme, preferred-mode switching distance.

1. Introduction

The use of multiple antennas at both ends of a wireless link has recently been shown to have the potential of drastically increasing spectral efficiency through a technique known as *spatial-multiplexing* [1]-[5]. This leverage often referred to as multiplexing gain permits the opening of multiple spatial data pipes between transmitter and receiver within the frequency of operation for no additional power expenditure, leading to a linear increase in capacity. Multiple antennas at both ends of a wireless link can also be used to improve link reliability through the use of *transmit diversity* techniques such as space-time coding [6]-[9], a leverage that is referred to as diversity gain. Diversity gain stabilizes the link and improves the quality of transmission. The multiplexing or diversity gain in multiple antenna systems depends strongly on the channel statistics which in turn depend on transmit and receive antenna spacing and the scattering environment. In practice, antenna spacing of tens of wavelengths at the base-station and up to a wavelength at the receiver is required in order to achieve significant multiplexing or diversity gain. Space to support multiple antennas is generally expensive or possible unavailable, more so at the subscriber unit than at the base-station. The use of polarization diversity, particularly dual-polarized antennas is a promising cost effective alternative where two spatially separated antennas can be replaced by a single antenna structure employing orthogonally polarized elements. In practice, it is not possible to exploit multiplexing gain and diversity gain simultaneously, due to the conflicting nature of these leverages and their methods of realization. Hence, it is important to understand and identify propagation conditions that suit one mode of transmission over the other [10].

Contributions. In this paper, we investigate the performance of uncoded spatial multiplexing and transmit diversity, in particular the *Alamouti scheme* [9] using data acquired from channel measurements. The data extracted from the channel measurements includes Ricean K-factor, cross-polarization discrimination (XPD) and fading signal correlation. We use previously developed performance analysis techniques to evaluate the performance of spatial multiplexing and the Alamouti scheme over a cell of radius 7 km for a fixed data rate and SNR at each location. Performance is measured in terms of average bit error rate (BER). The results indicate that if feedback regarding the channel statistics is available to the transmitter, appropriate selection of the transmission mode for a particular location can result in several orders of magnitude improvement in BER. Conveying channel statistics to the transmitter can be accomplished via low-bandwidth feedback and is much less complex than feeding back the channel state information itself, particularly in the fixed-wireless context. Additionally, the results

point to the existence of a preferred-mode switching distance within a cell - one mode of transmission is typically preferred over the other, depending on the subscriber's position relative to the preferred-mode switching distance.

Organization of the paper. The rest of this paper is organized as follows. Section 2 describes the system used and the setup for the measurement campaign. Section 3 reviews the channel model validated by the measurements. Section 4 briefly describes the performance analysis techniques used for spatial multiplexing and the Alamouti scheme. We present simulation results in Section 5. Finally, Section 6 contains our conclusions.

2. Measurement system and setup

2.1. Measurement system

A custom measurement system [11] was designed and implemented in hardware, which allowed the measurement of the complex channel response of a MIMO channel at 2.48 GHz center frequency.

The system was based on swept frequency sounding. A narrow-band test signal was swept in 200 KHz steps across a 4 MHz frequency band every 84 ms. The narrow-band receiver was swept synchronously with the transmitter, with timing references derived from rubidium clocks. The advantage of this design is a low noise floor (narrow bandwidth) and reduced complexity compared to spread spectrum measurement systems. Fig. 1 shows the configuration of the measurement system. Control and measurement signals were created using programmable RF signal generators. The recorded channel response data was streamed to computer hard disc for later processing using C++ and Matlab.

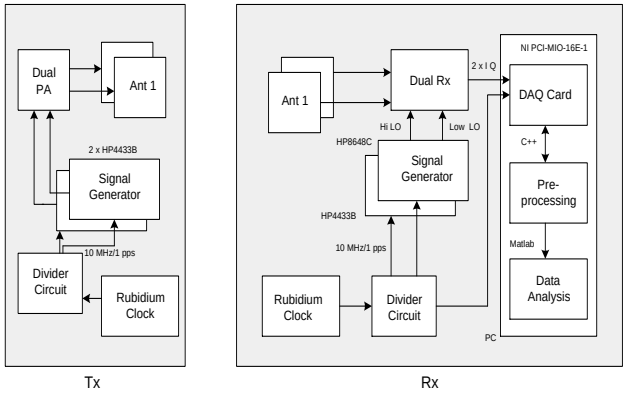

Figure 1: *Schematic of measurement system*

2.2. Measurement setup

In the measurements, a dual-polarized receive antenna with slanted polarizations (co-located $\pm 45^\circ$), a gain of 12 dBi and an azimuthal beam-width of 90° was used. It was mounted on a retractable mast of height 3 m. The $+45^\circ$ and -45° polarization transmit antennas separated by 10 wavelengths were also directive with an azimuthal beam-width of 90° and a gain of 17 dBi. Fig. 2 depicts the antenna configuration at transmitter and receiver for the measurement campaign. The transmitter was located on top of an office building with an antenna height of nearly 20 m above the street level.

Outdoor measurements of 58 fixed wireless locations with

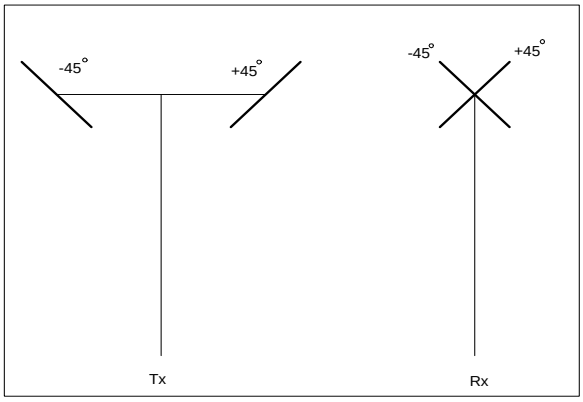

Figure 2: *Schematic of antenna configuration*

the receiver located at the curbside were conducted in the Bay Area over a cell of radius 7 km. At each location, two measurements 1 m apart were taken. Therefore, the total number of measurements was 116. Each measurement was taken over a 5 minute interval in the direction of the strongest signal which turned out to be the direct transmitter-receiver path in most cases. The terrain can be characterized as mostly suburban and flat with moderate tree and building density. The average building and tree height is about 15 m. Even at the cell edge, the received SNR when conducting the measurements was greater than 25 dB, ensuring high reliability of the channel statistics extracted from the measurements.

3. Channel model

In this section, we briefly discuss the narrow-band channel model [12, 13] that is validated by the measurements for the setup under consideration. The input-output relation for the channel model is given by

$$\boldsymbol{r} = \sqrt{E_s}\, \boldsymbol{H}\, \boldsymbol{x} + \boldsymbol{n},$$

where[1]

- $\boldsymbol{x} = [x_0 \;\; x_1]^T$ is the 2×1 transmit signal vector whose elements are taken from a finite (complex) constellation chosen such that the average energy of the constellation elements is 1,
- $\boldsymbol{r} = [r_0 \;\; r_1]^T$ is the 2×1 receive signal vector,
- $\boldsymbol{n}$ is the 2×1 complex-gaussian noise vector with $\mathcal{E}\boldsymbol{n} = 0$ and $\mathcal{E}\{\boldsymbol{n}\boldsymbol{n}^\dagger\} = \sigma_n^2 \boldsymbol{I}_2$,
- $\boldsymbol{H} = \begin{bmatrix} h_{0,0} & h_{0,1} \\ h_{1,0} & h_{1,1} \end{bmatrix}$ is the channel transfer matrix,
- E_s is the energy available at each of the transmit antennas.

The channel matrix $\boldsymbol{H}$ (also known as polarization matrix) describes the degree of suppression of individual co-and cross-polarized components, cross-correlation, and cross-coupling of energy from one polarization state to the other polarization state. The signals x_0 and x_1 are transmitted on the two different polarizations, and r_0 and r_1 are the signals received on the

[1]The superscripts ^{T} and † stand for transpose and conjugate transpose, respectively. $\mathcal{E}$ is the expectation operator and $\boldsymbol{I}_m$ is the identity matrix of dimension $m \times m$.

corresponding polarizations. We emphasize that the underlying channel is a $2-$input $2-$output channel, since each polarization mode is treated as a separate physical channel. The elements of $\boldsymbol{H}$ are (in general correlated) complex-gaussian random variables. Without loss of generality, the channel matrix may be expressed as the sum of a fixed (or sometimes of line-of-sight) component and a scattered (or variable) component as follows

$$\boldsymbol{H} = \sqrt{\frac{K}{1+K}}\overline{\boldsymbol{H}} + \sqrt{\frac{1}{1+K}}\boldsymbol{H'}, \quad (1)$$

where $\sqrt{\frac{K}{1+K}}\overline{\boldsymbol{H}}$ and $\sqrt{\frac{1}{1+K}}\boldsymbol{H'}$ are the fixed and scattered components of the channel matrix respectively. Hence,

$$\sqrt{\frac{K}{1+K}}\overline{\boldsymbol{H}} = \mathcal{E}\{\boldsymbol{H}\} \quad (2)$$

$$\sqrt{\frac{1}{1+K}}\boldsymbol{H'} = \boldsymbol{H} - \mathcal{E}\{\boldsymbol{H}\}. \quad (3)$$

The factors $\sqrt{\frac{K}{1+K}}$ and $\sqrt{\frac{1}{1+K}}$ in (1) are energy normalization factors and are related to the K-factor as will be described later. The elements of the matrix $\boldsymbol{H'}$, $h'_{i,j}$, are zero-mean complex-gaussian random variables whose variances depend on the propagation conditions. Throughout this paper, we assume

$$\mathcal{E}\{|h'_{0,0}|^2\} = \mathcal{E}\{|h'_{1,1}|^2\} = 1 \quad (4)$$

$$\mathcal{E}\{|h'_{0,1}|^2\} = \mathcal{E}\{|h'_{1,0}|^2\} = \alpha, \quad (5)$$

where α is directly related to the XPD (or separation of orthogonal polarizations) for the scattered component of the channel. Large XPD yields small α and vice versa. α is a function of the propagation environment (coupling between orthogonal polarizations due to scattering) and the ability of the antennas at the transmitter and receiver to separate orthogonal polarizations.

The elements of the matrix $\overline{\boldsymbol{H}}$, $\overline{h}_{i,j}$, do not vary with time and are arbitrary complex numbers satisfying

$$|\overline{h}_{0,0}|^2 = |\overline{h}_{1,1}|^2 = 1 \quad (6)$$

$$|\overline{h}_{0,1}|^2 = |\overline{h}_{1,0}|^2 = \alpha_F, \quad (7)$$

where α_F represents the XPD for the fixed component of the channel. For pure line-of-sight conditions (very high transmit and receive antennas), α_F unlike α is to a greater extent a function of the ability of the antennas at the transmitter and receiver to separate the orthogonal polarizations then it is of the scattering environment.

The K-factor of a fading channel is defined as the ratio of the power in the fixed component to the power in the scattered component. Under the assumptions made above, the K-factor for each element of the channel matrix, $K_{i,j}$, can be expressed as follows

$$K_{0,0} = K_{1,1} = K \quad (8)$$

$$K_{0,1} = K_{1,0} = \frac{\alpha_F}{\alpha}K, \quad (9)$$

where K is first alluded to in the energy normalization terms of (1). For the remainder of this paper, we shall refer to K as the K-factor of the system.

Recent literature in the area of MIMO technology assumes that the elements of the channel $\boldsymbol{H}$ are uncorrelated (i.i.d assumption). However, the experimental data reveals that it is not uncommon for the elements of $\boldsymbol{H}$ to be correlated. Since the coefficient of correlation between two random variables is shift invariant, it suffices to define the correlation coefficients between the elements of the zero-mean scattered component, $\boldsymbol{H'}$, as follows[2]

$$t = \frac{\mathcal{E}\{h'_{0,0}h'^*_{0,1}\}}{\sqrt{\alpha}} = \frac{\mathcal{E}\{h'_{1,0}h'^*_{1,1}\}}{\sqrt{\alpha}} \quad (10)$$

$$r = \frac{\mathcal{E}\{h'_{0,0}h'^*_{1,0}\}}{\sqrt{\alpha}} = \frac{\mathcal{E}\{h'_{0,1}h'^*_{1,1}\}}{\sqrt{\alpha}} \quad (11)$$

$$s = \mathcal{E}\{h'_{0,0}h'^*_{1,1}\} \approx \frac{\mathcal{E}\{h'_{0,1}h'^*_{1,0}\}}{\alpha}. \quad (12)$$

t is often referred to as the transmit correlation while r is referred to as the receive correlation. s in some sense is a combination of transmit and receive correlation. The approximation sign in (12) is based on measurement results. The experimental data gathered during the measurement campaign was used to extract values of K, α_F, α, r, t and s for each measurement location. Using these statistical parameters, it is possible to estimate the performance of spatial multiplexing and the Alamouti scheme in terms of average symbol error rate as will be described in the next section. It is pertinent to note that in addition to the channel statistics mentioned above, knowledge of the fixed component of the channel matrix, $\overline{\boldsymbol{H}}$, is required to estimate the symbol error rate. Due to limitations in the measurement equipment, determination of the phase information of $\overline{\boldsymbol{H}}$ was not possible. Instead, we resorted to random computer generated realizations of $\overline{\boldsymbol{H}}$ satisfying (6) and (7).

4. Performance analysis of spatial multiplexing and transmit diversity

4.1. Spatial multiplexing

Multiple antenna systems employ spatial multiplexing to maximize data rate transmitted to the user. Fig. 3 shows a schematic of a spatial multiplexing system for the dual-polarized antenna setup under consideration. The symbol stream to be transmitted is split into two sub-streams. The sub-streams are transmitted simultaneously by the transmitter, each sub-stream being launched on one of the orthogonal polarizations. We assume that the that the receiver has perfect channel knowledge and performs maximum-likelihood (ML) detection on the received signal vector to infer the transmitted symbols. It is possible to derive an average (averaged over the channel) scalar symbol error estimate, $\bar{P}_{mux}$, for spatial multiplexing as a function of the channel statistics as shown in [10, 13]. The method relies on a weighted average pairwise-error probability (PEP) approach and provides an estimate of the symbol error rate that matches the actual symbol error rate closely. Furthermore, $\bar{P}_{mux}$ reveals all the trends of the actual symbol error rate with varying channel statistics and SNR, eliminating the need for time-consuming computer simulations.

[2]The superscript * stands for complex conjugate.

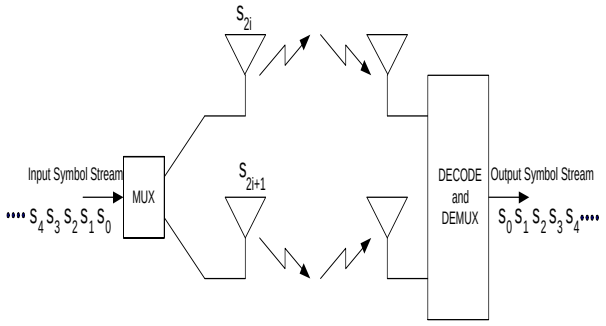

Figure 3: *Spatial multiplexing*

4.2. Alamouti scheme

Transmit diversity schemes exploit spatial diversity inherent in MIMO systems to improve link reliability. In this paper, we consider the performance of a simple transmit diversity scheme, the Alamouti scheme, for the polarization diversity channel under consideration. A schematic of the transmission strategy for the Alamouti scheme is shown in Fig. 8. Unlike the case for spatial multiplexing, redundancy must be introduced in the symbol stream to be transmitted to exploit spatial diversity. Thus, if symbols s_0 and s_1 are transmitted at $+45^\circ$ and -45° respectively during one symbol period, then during the following symbol period, symbols $-s_1^*$ and s_0^* are launched at $+45^\circ$ and -45° respectively. We assume that the receiver has perfect channel knowledge and performs ML detection on the received signal to determine the transmitted symbols. The ML receiver for the Alamouti scheme is much simpler than that for spatial multiplexing. This is due to the fact that the structure of the transmitted signal orthogonalizes the channel. Appropriate processing at the receiver effectively collapses the vector detection problem into simpler scalar detection problems. We derive an estimate of the average symbol error rate for the Alamouti scheme, $\bar{P}_{div}$, as a function of the channel statistics in [10]. Due to the scalar nature of the detection problem, the analysis is considerably simpler and less computationally intensive than that for spatial multiplexing. $\bar{P}_{div}$ reveals all trends of the actual symbol error rate and can predict performance of the Alamouti scheme accurately.

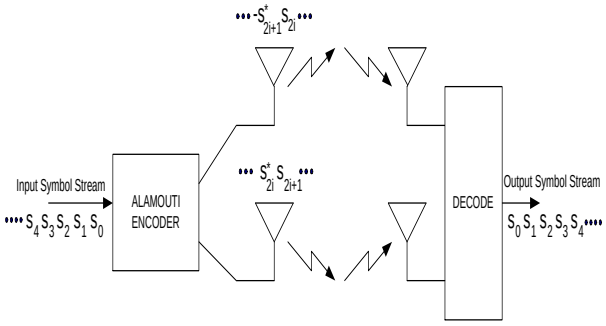

Figure 4: *Alamouti scheme*

5. Simulation results

Since the Alamouti scheme introduces redundancy in the transmitted data to exploit diversity, the data rate transmitted to the user for the Alamouti scheme will be half of the data rate for spatial multiplexing for the same underlying scalar constellation. In order to compare the schemes at the same data rate, we employ a higher order constellation for the Alamouti scheme in our simulations. In particular, we assume that transmitted symbols for spatial multiplexing are drawn from a 4-QAM constellation while the symbols for the Alamouti scheme are drawn from a 16-QAM constellation. This ensures that data is transmitted at 4 bits/symbol period for both schemes. Additionally, we assume an SNR of 20 dB at each location. Under our assumptions, the SNR is defined as $10\log_{10}\frac{2E_s}{\sigma_n^2}$. Furthermore, in order to compare the schemes based on BER we make the following approximations

$$BER_{mux} \approx \frac{\bar{P}_{mux}}{2} \quad (13)$$

$$BER_{div} \approx \frac{\bar{P}_{div}}{4}, \quad (14)$$

where BER_{mux} is the average bit error rate for spatial multiplexing and BER_{div} is the average bit error rate for the Alamouti scheme.

Fig. 5 shows the BER estimate for spatial multiplexing as a function of distance from the base-station. It is clear that BER_{mux} fluctuates widely over the cell, more so at greater distances from the base-station. The fluctuation can be attributed to the wide variation in channel statistics over the cell. Fig. 6 shows the BER estimate for the Alamouti scheme , BER_{div}, as a function of distance from the base-station. As for the case of spatial multiplexing, BER_{div} fluctuates widely over the cell.

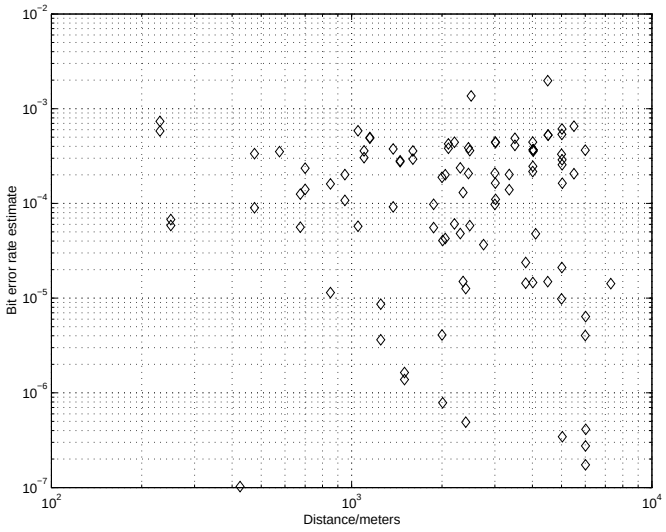

Figure 5: *BER estimate for spatial multiplexing*

From Fig. 5 and Fig. 6 it is clear that if knowledge of the channel statistics is available to the transmitter, the correct choice of transmission mode can result in up to several orders of magnitude improvement in BER. For example, consider the measurement location closest to the base-station (at a distance

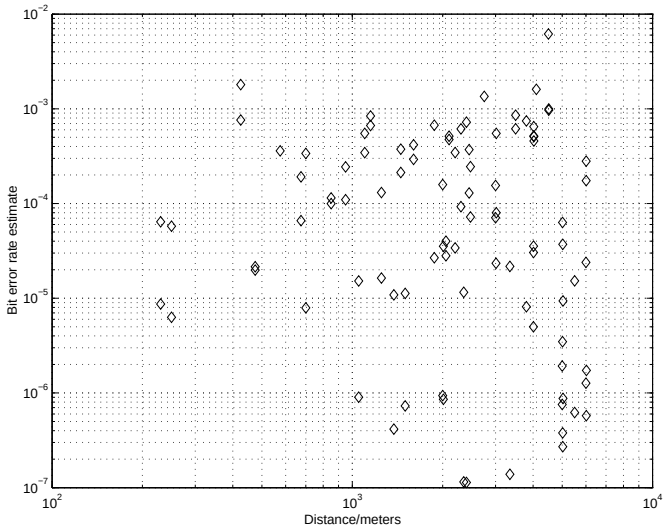

Figure 6: *BER estimate for Alamouti scheme*

of approximately 200 m). A comparison of the performance of the two schemes for this location reveals that the channel statistics at this point are much more conducive to the Alamouti scheme than they are for the spatial multiplexing. If feedback were available, the choice of spatial multiplexing over the Alamouti scheme would result in nearly two orders of magnitude improvement in performance. Fig. 7 shows the order of magnitude improvement in BER, $\frac{\max(BER_{mux}, BER_{div})}{\min(BER_{mux}, BER_{div})}$, possible through correct selection of the transmission mode for each measurement location. The plot clearly illustrates the value of feedback of channel statistics to the transmitter for mode selection. Feeding pertinent channel statistics back to the transmitter can be accomplished via a low-bandwidth link. Furthermore, conveying channel statistics to the transmitter is more easily accomplished than feeding back the channel state information itself, particularly in the fixed-wireless context.

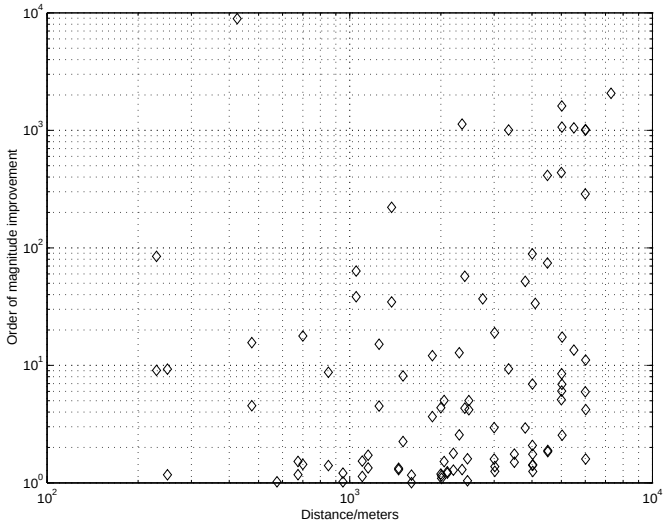

Figure 7: *Improvement in BER through optimal mode selection*

In the event that feedback is not available, it is beneficial to note the general trend in performance of spatial multiplexing and the Alamouti scheme over the cell area. In Fig. 8 we plot the least squares line fit for both spatial multiplexing and the Alamouti scheme data points. The plot reveals the existence of a switching point at about 1 km from the base-station. We refer to this distance as the preferred-mode switching distance – one mode of transmission is typically preferred over the other, depending on the user's position relative to the switching distance. We stress that choice of the transmission strategy based solely on the user's position relative to the preferred-mode switching distance may not be optimal. However, in the absence of feedback, the preferred-mode switching distance is a fair indicator of the preferred-mode of transmission. For the cell under consideration, spatial multiplexing is the preferred transmission strategy for locations that are less than 1 km away from the base-station, while the Alamouti scheme is preferred for locations closer to the cell edge. The preferred-mode switching distance for a cell will be a function of the SNR, data rate and the channel statistics inherent to the cell topology. The above simulations assume equal SNR at all locations within the cell. Alternatively, we can set the SNR at each location to be a function of the distance from the base-station and the path-loss exponent measured for the cell. Similar performance trend lines can be plotted for the two schemes for this scenario and a preferred-mode switching distance established.

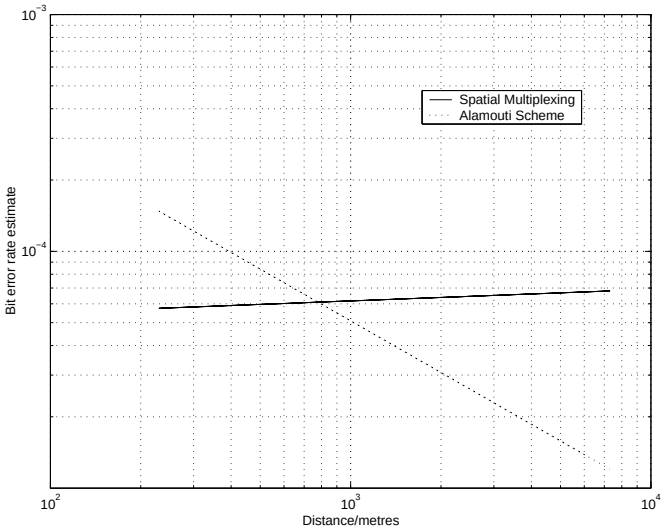

Figure 8: *Preferred-mode switching distance*

6. Conclusions

We studied the performance of spatial multiplexing and the Alamouti scheme in terms of average bit error rate for a dual-polarized antenna system for a fixed data rate and SNR over a cell of radius 7 km using data acquired through channel measurements. The results motivate the use of feedback of channel statistics to the transmitter for link adaptation. Appropriate choice of the transmission mode based on the channel statistics can improve the bit error rate by several orders of magnitude. Furthermore, the existence of a preferred-mode switching distance within the cell is established. For the cell under consideration, the channel statistics are more conducive to spatial multiplexing closer to the base-station, while the Alamouti scheme is preferred for locations closer to the cell edge.

7. References

[1] A. J. Paulraj and T. Kailath, "Increasing capacity in wireless broadcast systems using distributed transmission/directional reception," *U.S. Patent*, No. 5,345,599, 1994.

[2] I. E. Telatar, "Capacity of multi-antenna Gaussian channels," Tech. Rep. #BL0112170-950615-07TM, AT&T Bell Laboratories, 1995.

[3] G. J. Foschini and M. Gans, "On limits of wireless communications in a fading environment when using multiple antennas," *Wireless Personal Communications*, vol.6, no.3, pp.311-335, March 1998.

[4] G. J. Foschini, "Layered space-time architecture for wireless communication in a fading environment when using multi-element antennas," *Bell Labs Tech. J.*, pp.41-59, Autumn 1998.

[5] H. Bölcskei, D. Gesbert and A. Paulraj, "On the capacity of OFDM-based spatial multiplexing systems," *IEEE Trans. Comm.*, in press.

[6] J. Guey, M. Fitz, M. Bell, and W. Kuo, "Signal design for transmitter diversity wireless communication systems over Rayleigh fading channels," *Proc. IEEE VTC*, pp.136-140, 1996.

[7] V. Tarokh, N. Seshadri, and A. R. Calderbank, "Space-time codes for high data rate wireless communication: Performance criterion and code construction," *IEEE Trans. Inf. Theory*, vol.44, pp.744-765, March 1998.

[8] V. Tarokh, H. Jafarkhani, and A. R. Calderbank, "Space-time block codes from orthogonal designs," *IEEE Trans. Inf. Theory*, vol.45, pp.1456-1467, July 1999.

[9] S. M. Alamouti, "A simple transmit diversity technique for wireless communications," *IEEE J. Sel. Areas Comm.*, vol.16, pp.1451-1458, October 1998.

[10] R. Nabar, H. Bölcskei, V. Erceg, D. Gesbert and A. Paulraj, "Performance of multi-antenna signaling strategies in the presence of polarization diversity," *IEEE J. Sig. Processing*, to be submitted, 2001.

[11] D. Baum, D. Gore, R. Nabar, S. Panchanathan, K. V. S. Hari, V. Erceg, and A. J. Paulraj, "Measurement and characterization of broadband MIMO fixed wireless channels at 2.5 GHz," *IEEE Int. Conf. on Personal Wireless Comm.*, pp.203-206, Dec. 2000.

[12] V. Erceg, D. S. Baum, S. Pitchaiah, A. J. Paulraj, "Capacity obtained from multiple-input multiple-output channel measurements in fixed wireless environments at 2.5 GHz", *IEEE GLOBECOM*, submitted, 2001.

[13] H. Bölcskei, R. Nabar, V. Erceg, D. Gesbert and A. Paulraj, "Performance of spatial multiplexing in the presence of polarization diversity," *ICASSP 2001*, May 2001.